Experimental Analysis And Parameter Optimization On The Reduction of NOx From Diesel Engine Using RSM And ANN Model

Maheswari Chenniappan (maheswarikec@gmail.com)
Kongu Engineering College https://orcid.org/0000-0002-9896-6553
Ramya A S
Sanskriti Group of Institutions
Baskar Rajoo
Kongu Engineering College
Selvakumar Nachimuthu
Kongu Engineering College
Rishab Govind Rajaram
Kongu Engineering College
Vasanth Malaichamy
Kongu Engineering College

Research Article

Keywords: Air pollution control, Artificial neural network (ANN), Dielectric Barrier Discharge (DBD), NOx reduction, Nonthermal Plasma (NTP), Response surface method (RSM)

Posted Date: September 3rd, 2021

DOI: https://doi.org/10.21203/rs.3.rs-826968/v1

Experimental analysis and parameter optimization on the reduction of NOx from diesel engine using RSM and ANN Model

Maheswari Chenniappan[1], Ramya A S[1*], Baskar Rajoo[1], Selvakumar Nachimuthu[1], Rishab Govind Rajaram[1], Vasanth Malaichamy[1]

[1]Kongu Engineering College, Perundurai, Erode-638060, Tamilnadu, India.

[2]Sanskrithi School of Engineering, Puttaparthi, Ananthapur-515134, Andhra Pradesh, India. Corresponding author email: ramya24591@gmail.com

Abstract

The feasibility of the Non-thermal Plasma (NTP) process is examined by four operating parameters including NOx concentration (300-400 ppm), gas flow rate (2-6 lpm), voltage (20-30 kV) and electrode gap (3-5 mm) using a Dielectric Barrier Discharge (DBD) reactor for removing NOx from diesel engine exhaust. Based on the NTP study, the NOx removal efficiency and energy efficiency of the NTP reactor are measured. Optimization of process parameters have been carried out using response surface-based Box Behnken Design (BBD) method and Artificial Neural Network (ANN) method. ANN based optimization is carried out using feed-forward network algorithm which has 4 input nodes, 10 hidden nodes and 2 output nodes. Based on the RSM and ANN model study, R^2 value are obtained as 0.98 and 0.99 respectively. These models demonstrates that they have strong agreement with the experimental results. The results are indicated that the RSM model's optimum conditions resulted in a maximum NOx reduction of 60.5% and an energy efficiency of 66.24 g/J. The comparison between the two models confirmed the findings, whereas this ANN model displayed a stronger correlation to the experimental evidence.

Keywords: Air pollution control; Artificial neural network (ANN); Dielectric Barrier Discharge (DBD); NOx reduction; Nonthermal Plasma (NTP); Response surface method (RSM);

Introduction

Since the second half of the 20th century, global warming has gained the status of a major concern due to a rise in the earth's temperature. In one third of the United States, pollution has greatly increased, allowing gases to enter the atmosphere and due to this, global warming has accelerated at a much greater rate. Around 40% of NOx emissions are due to vehicle use of the road. Emissions of gases such as sulphur oxides, nitrogen oxides and carbon monoxide contribute to toxicity, which has both human and environmental consequences (Chen &Liu 2010, Kampa &Castanas 2008). Release of NOx among these gases has a significant impact on environmental degradation. The cause of NOx pollution is automotive exhausts, exhaust gases generated in industries like turbines, power plants and cement kilns (Amoatey et al. 2019, Sohn et al. 2021). When combustion occurs at high temperature, NOx is likely to be formed. Oxidation of nitric oxide (NO) results in the production of a tropospheric greenhouse gas with a strong odor. These exhaust sources, while feasible in theory, are still challenging to get rid of the NOx entirely (Maheswari 2014, Li et al. 2011). There is a need for an efficient method for reducing the amount of NOx emitted by these sources.

The Indian government strongly demands that diesel generator manufacturers adhere to the permissible NOx and hydrocarbon emission limits in the atmosphere. With respect to commercial vehicles, India's National Emission Standards-EU has proposed a drop from 0.39 grams of hydrocarbon emission limits per kilometre in 2017 to 0.20 grammes of NOx limits in 2020 as illustrated in Fig. 1a. There are over a million vehicles sold in the commercial vehicle sector for the first time in the fiscal year, an all-time high level of production for Indian trucks and buses in 2019. The most rapid growth in the year is for heavy trucks. As shown in Fig. 1b, according to the Central Pollution Control Board (CPCB), 3.5 g/kmHr of NOx is emitted into the atmosphere in 2020 as a result of heavy diesel vehicles (Source CPCB, 2020).

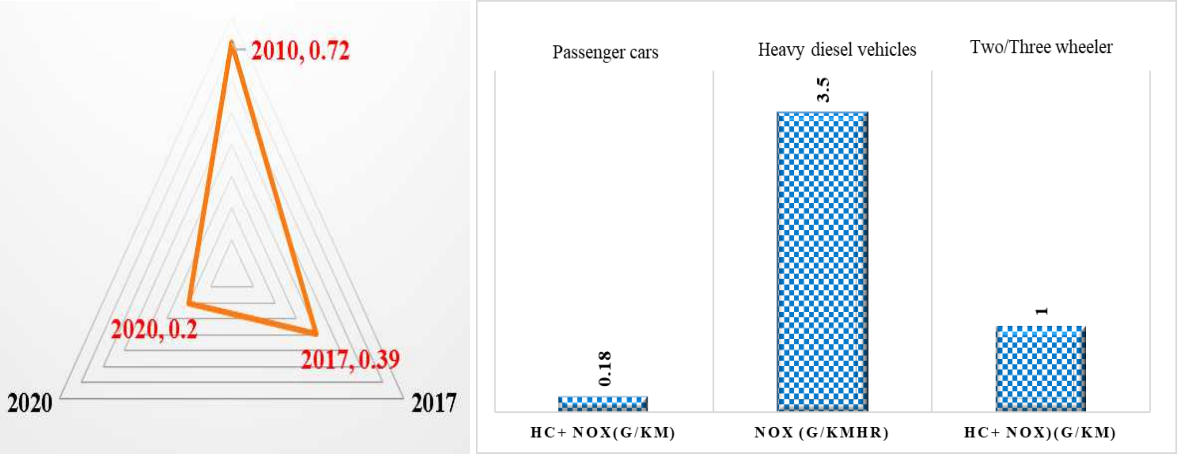

Fig. 1 Emission control standards a. light commercial vehicles and b. emission norms for different vehicles (Source: CPCB-India,2020)

The use of emerging technology and improvements to existing techniques have become needed to confront the constraints on NOx pollution. Selective of non-catalytic reduction (SCR) is commonly used nowadays, especially for reducing NOx emission during coal combustion. Several other methods, such as mechanical scrubbing, adsorption, absorption, electron beam, electrochemical cell or vapour diffusion are often used (Arun kumar 2019, Maheswari 2013, Skalska et al. 2010). Nonetheless, each of these techniques has its limits and drawbacks. Additionally, certain developing nations have placed highly stringent limits on NOx emissions (Maheswari et al. 2017). As a result, research is being conducted worldwide to develop more reliable approaches. Plasma-assisted deletion is an important and superior suggested approach for cleaner air among NOx pollution control techniques (Tang et al. 2021). Removal of nitrogen oxides using Nonthermal Plasma (NTP) has been put forward as a viable option (Takaki et al. 2004). In the NTP systems, toxins are easy to remove, there are no organic contaminants and maintenance costs, and primary processing is at ambient pressure (Suresh et al. 2021a, Suresh et al. 2021b).

In view of the benefits of NTP, even though the treatment efficiency of NOx reduction is substantial, the key difficulty of using this technology is energy consumption. Many parameters, such as initial concentration of NOx, gas flow rates, treatment time, duty cycle, electrode gap, electrode geometry and applied voltage will affect purification

performance and energy rate of plasma system (Kuwahara et al. 2016, Mizuno 2007, 2013, Takaki et al. 2004). In the present study, the Dielectric Barrier Discharge (DBD) based NTP reactor is developed to reduce the NOx which will clearly provide a homogeneous, low-energy top-discharge with higher efficiency when placing dielectric material between the high-voltage and ground electrodes (Ansari et al. 2020, Khan &Kim 2020). NTP tends to be more ideal for the removal of NOx due to its ability to efficiently convert nitrogen to OH radicals and the ease of installation, increasing the risk of the formation of free radicals, such as hydroxyl radical (OH) (Krosuri et al. 2021). Electrons with energy ranges from 1 to 10 eV are emitted during plasma process and exposed to nitrogen in gases to process nitric oxide to nitrogen dioxide (Tang et al. 2021). Zhu et al. (2020) found an alternative approach that used the DBD. Only ammonia is used to make DBD radicals, which are combined with the flue gases to start a reaction. The removal efficiencies ranged between 93.89% and energy density of 500 J/lit.

Exhaustive simulation and process optimization efforts have been devoted to understanding the system behavior and finding the global optimal for chemical processes so far and some have used the statistical simulation approach like mathematical modeling, Response surface methodology (RSM) and Artificial Neural Network (ANN) (Bhatti et al. 2011, Zhao et al. 2020). Each approach has its own set of benefits and drawbacks. Mathematical modelling, for example, involves a system comprehension that includes functions that apply to the system. It can contain calculations, equations, constitutive equations and restrictions. The consistency of the model works relatively well when the dependent and independent variables maintain a constant relationship, but decreases dramatically when the equation exhibits nonlinear behavior (Chen &Tan 2012). Other tools, such as RSMs or ANNs, have been used with nonlinear systems to see how input variables impact the behavior of the system (Zhao et al. 2020). The DOE research will investigate all the independent variables within the bounds of each variable and integrate the data. Out of all techniques, in specific, RSM has actually been used in numerous technical fields.

Complex activities like learning and pattern recognition have given rise to a vast quantity of computational investigation into small networks of basic components termed ANNs. In the last few years, scientists in a number of scientific fields have taken an interest in the possible mathematical usefulness of artificial intelligence techniques to tackle a number of issues. While ANNs are designed to help understand the roles of the brain in mammalian. Additionally, ANNs are used to render an approximation of hidden feature. It's quite powerful for managing very subjective data, particularly in those areas where analysis is essential. Other methods of neural network creation are in progress, in addition to ANN. To name a few, feed-forward networks and real-time control systems are adopted as well as an adaptive neural network is applied to systems that needed it (Agatonovic-Kustrin &Beresford 2000, Picos-Benítez et al. 2017, Zhao et al. 2020).

The purpose of this work is to develop a DBD reactor with a larger efficiency for eliminating NOx. To enhance the reactor efficiency of removing NOx, four parameters are analyzed via BBD design: the initial NOx concentration, gas flow rate, electrode gap and voltage. Additionally, the energy efficiency of the DBD rector is evaluated. The artificial neural network (ANN) uses both inter-variable interactions as well as both interactive factors

in predicting and simulating interrelationships. This is used to determine the predictor importance of the resulting model.

Experimental Methodology

Experimental setup

The schematic experimental setup for NOx reduction is illustrated in Fig. 2 and its specifications are mentioned in the previous study (Suresh et al. 2021b). This design is comprised of four main elements: gas supply, DBD reactor, power supply module and gas-sensing apparatus. A graphical representation of the DBD reactor is shown in Fig. 2. Inner electrode has the dielectric shielding placed inside the reactor. The outer electrode is constructed from copper wires that is fixed to the dielectric layer. Stainless steel is used as the grounding electrode. Due to the existence of large electrical foils (centroids) in the middle of the dielectric tubes, flashover is avoided by using foil sides that is lower in voltage. In the reactor, glass used as the dielectric barrier. Surface thickness of all components is 2 mm, as is shown as a strong dielectric tube in Fig. 2. The reactor is attached to a high voltage supply to produce plasma that should be with peak intensity. Fluidised gases are introduced by a nozzle into the reactor. The specific quantity of NOx and oxygen are mixed thoroughly and entered into the DBD reactor. To measure the inlet and outlet NOx concentrations, the NOX sensor with transmitters is fixed. The flue gas from the diesel engine containing nitrogen oxide (NOx) is mixed with 10% oxygen (O_2) and then it is injected to the reactor. By using air flow regulator, the mixture gas flow rate is regulated. Based on the NOx level in the untreated air, the NOx sensor is used to determine the NOx level. DAQ is the data acquisition card that is used to retrieve sensor (NOx) data and pass control signals to the ultimate feedback controller. NOx emissions are detected and regulated using a customized ADu841 VVME processor-based VMAT DAQ card.

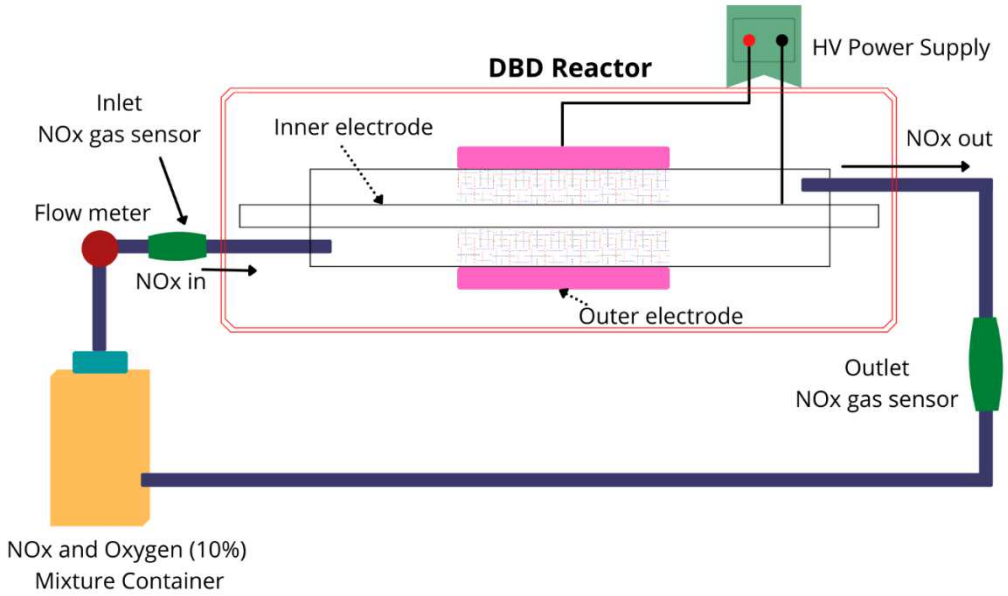

Fig. 2 Experimental setup for NOx reduction

RSM modeling

Experimental conditions are determined using the RSM and planning technique that decreases the workload significantly while still obtaining an optimal model result. One of the main operations in process optimization design studies, the Box Behnken Design (or BBD), describes how much more improvements in production output or efficiency can be attained by the process as well as the conditions in which it can be carried out (Srikanth et al. 2021). For the experimental layout, Minitab 18 software is being used. Four parameters and three stages are involved in the BBD configuration. As seen in Table 1, the independent variables are NOx initial concentration, gas flow rate, high voltage and electrode gap and respective values have been labeled as: +1, 0, -1, and thus the response variable being NOx reduction and reactor energy efficiency. Experimental runs included 27 runs which typically consisted of three attempts each to correct and/prove an error before they are incorporated into the calculations to determine experimental error (Table 2).

Table 1 Experimental ranges for the BBD system.

Variables	Ranges		
	low	centre	high
A: NOx Concentration (ppm)	300	350	400
B: Flow rate (lpm)	2	4	6
C: Voltage (kV)	20	25	30
D: Electrode gap (mm)	3	4	5

129 **Table 1** Experimental results as per BBD design

Run order	Factors				Actual		BBD Predicted		BBD Error (%)		ANN Predicted		ANN Error (%)	
	A	B	C	D	Nox Reduction (%)	Energy Efficiency (g/J)	Nox Reduction (%)	Energy Efficiency (g/J)	Nox Reduction (%)	Energy Efficiency (g/J)	Nox Reduction (%)	Energy Efficiency (g/J)	Nox Reduction (%)	Energy Efficiency (g/J)
1	300	2	25	4	54.6	26.21	53.16	23.54	2.64	10.18	54.901	26.65	-0.55	-1.68
2	400	2	25	4	47.5	30.4	46.99	29.94	1.08	1.51	47.564	30.316	-0.13	0.28
3	300	6	25	4	37.2	53.65	37.48	54.66	-0.74	-1.87	37.163	53.735	0.10	-0.16
4	400	6	25	4	26.4	50.76	27.61	53.97	-4.56	-6.33	26.489	50.767	-0.34	-0.01
5	350	4	20	3	38.9	54.48	39.39	53.78	-1.26	1.29	36.45	54.161	6.30	0.58
6	350	4	30	3	48.3	45.09	49.04	46.49	-1.54	-3.10	48.188	45.023	0.23	0.15
7	350	4	20	5	33.8	47.32	33.56	47.38	0.72	-0.13	33.848	47.286	-0.14	0.07
8	350	4	30	5	43.7	40.78	43.21	40.09	1.13	1.69	43.706	40.731	-0.01	0.12
9	300	4	25	3	47.3	45.4	46.56	45.74	1.56	-0.74	47.293	45.413	0.01	-0.03
10	400	4	25	3	38.1	48.76	38.54	48.59	-1.16	0.34	38.009	48.724	0.24	0.07
11	300	4	25	5	40.1	38.49	40.73	39.34	-1.57	-2.21	39.334	39.215	1.91	-1.88
12	400	4	25	5	31.6	40.44	32.71	42.20	-3.51	-4.35	31.587	40.476	0.04	-0.09
13	350	2	20	4	44.8	31.36	40.88	33.35	8.75	-6.35	44.751	31.416	0.11	-0.18
14	350	6	20	4	29.6	62.03	29.38	60.93	0.74	1.78	27.731	62.028	6.31	0.00
15	350	2	30	4	56.4	26.32	56.56	26.06	-0.29	0.98	56.376	26.364	0.04	-0.17
16	350	6	30	4	40.4	56.56	39.03	53.64	3.39	5.17	40.602	56.756	-0.50	-0.35
17	300	4	20	4	39.7	47.64	38.82	46.18	2.22	3.06	39.663	47.501	0.09	0.29
18	400	4	20	4	31.8	50.88	30.80	49.04	3.14	3.61	31.941	50.908	-0.44	-0.06
19	300	4	30	4	46.2	36.96	48.47	38.89	-4.91	-5.23	53.131	36.939	-15.00	0.06

20	400	4	30	4	41.5	44.26	40.45	41.75	2.53	5.67	41.091	42.631	0.99	3.68
21	350	2	25	3	55.3	30.97	54.66	32.90	1.16	-6.25	55.468	32.719	-0.30	-5.65
22	350	6	25	3	36.4	61.25	37.12	60.48	-1.98	1.26	36.371	61.19	0.08	0.10
23	350	2	25	5	48.3	27.05	48.82	26.51	-1.08	2.00	48.289	27.177	0.02	-0.47
24	350	6	25	5	31.8	53.5	31.29	54.08	1.61	-1.09	31.777	53.455	0.07	0.08
25	350	4	25	4	41.6	46.59	41.30	46.93	0.72	-0.74	41.531	46.653	0.17	-0.13
26	350	4	25	4	41.6	46.59	41.30	46.93	0.72	-0.74	41.531	46.653	0.17	-0.13
27	350	4	25	4	41.6	46.59	41.30	46.93	0.72	-0.74	41.531	46.653	0.17	-0.13

130

The NOx elimination BBD model displayed an association between independent variable as a secondary response surface model. Following equation (Eq 1) demonstrates the relationship between independent and dependent variables,

$$Y_0 = \delta_0 + \sum_{i=1}^{k} \delta_i X_i + \sum_{i=1}^{k} \delta_{ii} X_i^2 + \sum_i \sum_{<j=2}^{k} \delta_{ij} X_i X_j + \vartheta_i \quad (1)$$

Where, Y_0 denotes the predicted variable response, X_i and X_j denotes independent variables, δ_i, δ_{ii} and δ_{ij} denotes the i^{th} linear, quadratic and interaction coefficients and $\vartheta_i$denotes the error. The original concentration of NOx pumped into the reactor is referred to as NO_{in}, while the concentration of NOx at the reactor's vent or exit is referred to as NO_{out}. As seen in equation (Eq 2), NOx removal is measured in ppm (parts per million).

$$NOx\ removal\ (\%) = \frac{NO_{in} - NO_{out}}{NO_{in}} X100 \quad (2)$$

The most commenly used metrics for measuring non-thermal plasma energy consumption are power density and energy efficiency, which are determined using the following equations (Eq 3-4) (Mansouri et al. 2020, Suresh et al. 2021b).

$$Power\ density\ (J/lit) = \frac{Power\ (W) * 60}{Gas\ flow\ rate\ (lpm)} \quad (3)$$

$$Energy\ Efficiency\ (g/J) = \frac{NO_{in} - NO_{out}}{Power\ density} \quad (4)$$

ANOVA is a form of analysis of variance that is employed in statistics, which looks for the combination of internal variability (randomness) and underlying trends (systematic) variables that accounts for the total variability discovered in the study. Statistical variables may or may not affect the given results, depending on whether they are systematically distributed. This statistical analysis helps researchers estimate the effect that the study variables have about the results of a study's dependent variable (McHugh 2011). When forecasting the result of the given occurrence, the coefficient of determination would be a mathematical calculation that evaluates the extent to which variations throughout one parameter could be justified by differences in another variable. In other words, this coefficient, more often referred to as R-squared (R^2), quantifies the strength of a linear interaction between two variables and has been heavily used by researchers when doing pattern analysis (Armstrong et al. 2002, Keselman et al. 1998). To understand the significance of the effect of the responses to be assessed, ANOVA has been used. In accordance with the quadratic model calculation, 2-based contour plots are created and they have been used to arrive at conclusions regarding the influence of each parameter as well as to examine the interplay between them (Zwanenburg et al. 2011).

ANN modeling

ANN has a biological analogy for the fundamental concept of a highly flexible and effective computer device. The network consists of several interconnected units to allow for data communications between them. These units are basic

generators which run in parallel. They also are called nodes or neurons (Agatonovic-Kustrin &Beresford 2000). Each neuron is linked by a communication connection to another neuron. Each link has been linked to a weight that provides information on the input signal. This has been the most helpful input for the resolution of a specific problem by neurons since the weight normally stimulates or prevents the signal. The internal condition of each neuron has been known as a signal stimulation. Some signals are produced after being combined with an input rule; and signals resulting from combining the two would always be transmitted to other units (Agatonovic-Kustrin &Beresford 2000, Elmolla et al. 2010).

A back-propagation trained model is used for the neural network. Neural background nets with a single hidden layer are shown to provide reliable approximations to any continuous function if adequate hidden neurons are present. One essential aspect of back propagation neural networks has been that the relations among different variables are not defined. Instead, they benefit from the explanations that are shown to them. Additionally, individuals are capable of generalizing accurate answers one that superficially mimic the information used during the learning process (Civelekoglu et al. 2009, Sakiewicz et al. 2020).

Modeling the ANN framework is done using the same dataset that is used for the modelling of RSM is one of the exercises is a major upgrade in the RSM model. Based on experimental results (Table 2), numerical and numerical prediction, a full model is created to forecast the NOx reduction (using the MathWorks' MATLAB programme). The application used a 3-layered neural network. There have been four input nodes, ten hidden nodes and two output nodes as illustrated in Fig. 3. A back propagation algorithm based on the Levenberg–Marquardt principle with a sigmoidal function has been introduced. The experimental neurons contained an NOx concentration, flow rate, voltage and electrode gap, which are each fed into the evaluate to calculate the output NOx reduction and energy efficiency.

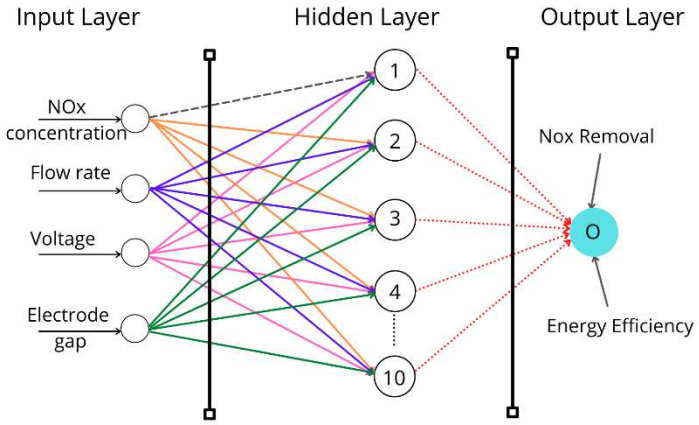

Fig. 3 ANN model structure

Model validation using RSM and ANN

The coefficient of determination (R^2), the adjusted R^2 value and the mean squared error are used to measure and equate the RSM and ANN models' accuracy. Equations (Eq 5-8), characterise MSE, RMSE, MAPE and R^2, respectively (Kim et al. 2019, Soleimanzadeh et al. 2019).

188 $$MSE = \frac{\sum_{i=1}^{n}(E_i - Y_i)^2}{n} \quad (5)$$

189 $$RMSE = \sqrt{\frac{\sum_{i=1}^{n}(E_i - Y_i)^2}{n}} \quad (6)$$

190 $$MAPE = \frac{\sum_{i=1}^{n}|E_i - Y_i/E_i|}{n} X\ 100 \quad (7)$$

191 $$R^2 = 1 - \frac{\sum_{i=1}^{n}(E_i - Y_i)^2}{\sum_{i=1}^{n}(E_i - E_m)^2} \quad (8)$$

192 The residuals, E_i, is the variance between the observed response. If the estimates from the model matched the
193 experimental values exactly, R^2 is equal to 1.0. The R^2 is a slightly changed abbreviation of the original that
194 incorporates the number of predictors. From Equation (Eq 5-8), n denotes number of trials, Y_i denotes predicted
195 response and E_m denotes average observed response.

196 **Results and Discussion**

197 **RSM modeling**

198 **Model validation**

199 Table 3 shows the experimental outcomes achieved by BBD model and reasonably similar the calculated data of the
200 3 replicated groupings showing the data are reproducible properly. Predicted accuracy and error rates and the
201 experiment shows agreement with the results, thereby proving that the prediction works. The discrepancy between the
202 expected values and the actual value is lower than 2, which means that data fits as predicted. To determine the factors
203 to be tested, the design is built using the second-order polynomial model. NOx concentration (A), flow rate (B),
204 voltage (C) and electrode gap (D) are used as independent inputs to determine the dependent variable includes NOx
205 reduction and energy efficiency. The equation (Eq 9-10) is effective for characterizing the effect of each variable's
206 coefficient

$$\text{Nox Reduction (\%)} = -13.4 + 0.423\ A - 4.49\ B + 0.9650\ C - 2.917\ D - 0.000666\ AXA + 0.418\ BXB - 0.00925\ AXB \quad (9)$$

$$\text{Energy Efficiency (g/J)} = -143.5 + 0.930\ A + 19.97\ B - 0.729\ C - 3.197\ D - 0.001186\ AXA - 0.860\ BXB - 0.01770\ AXB \quad (10)$$

207

208 The above results show the model's quadratic coefficient of flow rate to have the most beneficial effect on NOx
209 elimination with its maximum negative coefficient and energy efficiency with its maximum positive coefficient. This
210 is due to the decrease in NOx from increasing the gas flow rate, while the energy efficiency is enhanced by the rise in
211 the flow rate. The negative symbol for the electrode gap is the second most important variable to reduce the reduction
212 of NOx and energy efficiency by increasing the flow rate. Similar results are obtained by Mansouri et al. (2020) in the
213 experiment of the NOx reduction by packed bed DBD reactor.

The normal test plot has been used to see whether results follow the bell curve or the normal distribution. According to Fig. 4a and b, the residuals are closely compared to the linear line and ranged between – 2 and 2 in terms of NOx reduction and -4 to 4 in terms of energy efficiency. The Pareto chart shows the prevalence of defects and also its overall effect, which would also be usually referred to as a bar chart. It would be very helpful to use pareto charts to identify flaws in order to locate the most prevalent elements of the model. From Fig. 5, the bars are listed from largest to smallest in ascending order (from tallest to shortest). The size of the largest bar represents the most critical aspect of the response. Fig. 5a illustrates the pareto curve for NOx reduction, indicating that the most critical element is gas flow rate, followed by voltage, NOx concentration, and electrode gap. Similar to that is shown in Fig. 5b, the gas flow rate has the highest influencing factor compared to voltage, electrode gap and NOx concentration being taken into consideration when measuring performance**.**

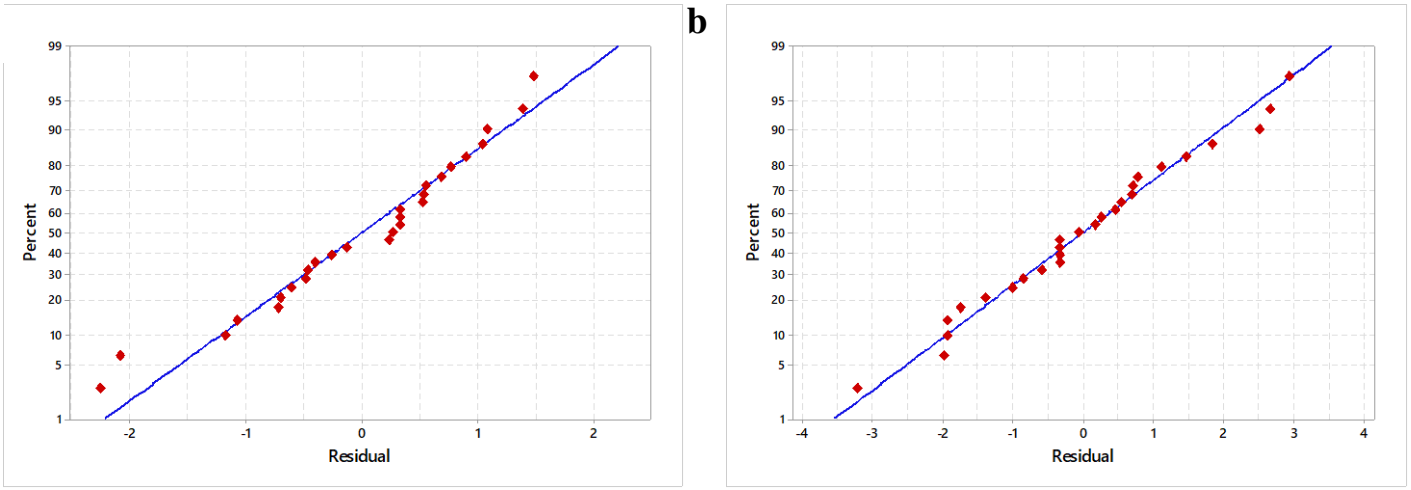

Fig. 4 Normal plot a. NOx reduction and b.Energy Efficiency

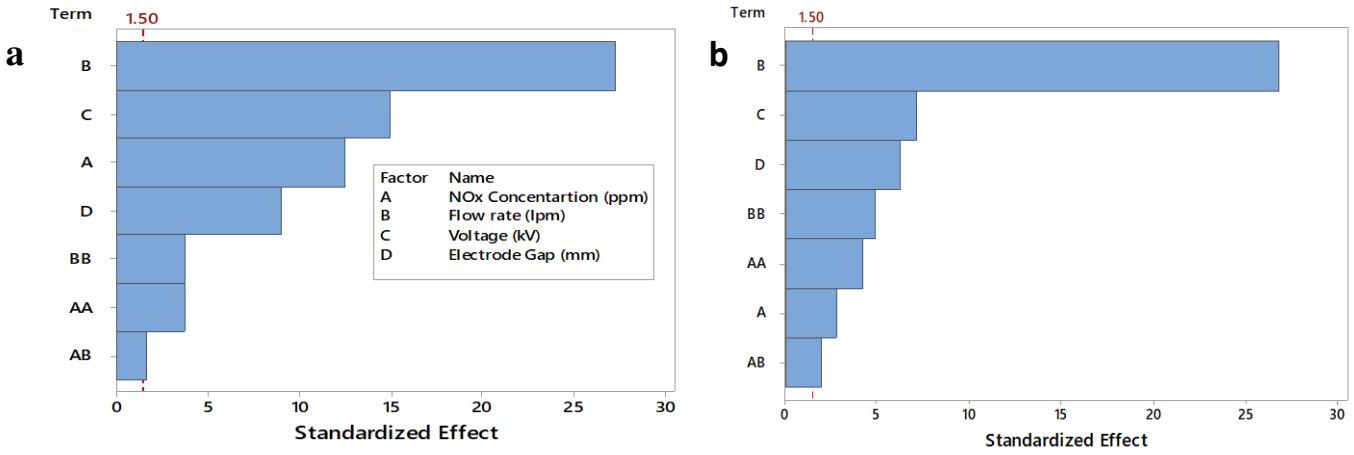

Fig. 5 Pareto plot a. NOx reduction and b. Energy Efficiency

ANOVA analysis

Tables 3 and 4 demonstrate the ANOVA findings for the BBD model for NOx reduction and energy efficiency, respectively. The data illustrate the SS (Sum of Squares), DF (degree of freedom), MS (Mean square), F value and

probabilities (p value) for all the linear and quadratic parameters. The studies have been performed to see the impact of both of individual factors as well as the synergistic ones as in BBD model is of several factors.

Table 4 displays the NOx reduction ANOVA effects of the BBD model. Many of the linear terms includes NOx concentration, flow rate, voltage and electrode gap in the RSM model had p values below 0.0001, which implies that they are important to the model. The most important of the four factors is in particular the gas flow rate which is contributed 58.74% in NOx reduction. By examining the ANOVA table 4, thus learn how often independent variables impact on the reduction of NOx. By analyzing the significance level of the variables' quadratically terms, are observed that the model is applicable to $A^{2,}$ $B^{2,}$ C^2 and D^2. The model should be subjected to the following conditions: F > 0.1, R-sq > 0.95, R-sq (pred) > 0.7 and R-sq (adj)- R-sq (pred) < 0.2. P-value and f-value is employed to validate the model. From Table 3, the fit of this model is good in the regression field, the F value of the model is 71.62 with $p < 0.0001$. R-sq value of 0.9882, R-sq (pred) of 0.9319 and R-sq (adj)- R-sq (pred) of 0.0425 demonstrating a high level of consistency and credibility.

Similarly, the Table 4 presented the ANOVA effects of energy efficiency in BBD model. The contribution of the overall model is greater than that is stated here, with a p value of <0.0001, which implies that the variables do significantly impact the response. According to the model, the NOx concentration, flow rate, voltage and electrode gap (linear terms) had a significant effect on energy efficiency of DBD reactor. Out of these factors, flow rate has a major significant one which contributes 82.33% for energy efficiency. The initial NOx concentration and flow rate affected the energy efficiency of DBD reactor, which is quadratic rather than linear. From Table 4, the fit of this model is good in the regression field, the F value of the model is 122.18 with $p < 0.0001$. R-sq value of 0.9783, R-sq (pred) of 0.9357 and R-sq (adj)- R-sq (pred) of 0.0346 demonstrating a high level of consistency and credibility. Fig. 6 shows a close association between the previsied and real values with the R^2 high coefficient value of 0.9788 for the reductions in NOx and energy efficiency. So as a result, measurement established a reasonable expectation of the expected response within the scope of the study.

Table 2 ANOVA results for the NOx reduction

Source	DF	Adj SS	Adj MS	F-Value	P-Value	Remarks
Model	14	1548.49	110.607	71.62	<0.0001	Highly significant
A	1	193.60	193.603	125.36	<0.0001	Highly significant
B	1	920.50	920.501	596.03	<0.0001	Highly significant
C	1	279.37	279.367	180.89	<0.0001	Highly significant
D	1	102.08	102.083	66.10	<0.0001	Highly significant
A X A	1	17.04	17.041	11.03	0.006	Significant
B X B	1	12.81	12.813	8.30	0.014	Significant
C X C	1	0.12	0.120	0.08	0.785	Significant
D X D	1	0.61	0.608	0.39	0.542	Significant

Error	12	18.53	1.544			
Lack-of-Fit	10	18.53	1.853	5.24	0.345	Not Significant
Total	26	1567.03				

S	1.2427
R-sq	0.9882
R-sq (adj)	0.9744
R-sq (pred)	0.9319

267

268 **Table 3** ANOVA results for the energy efficiency

Source	DF	Seq SS	Adj MS	F-Value	P-Value	Remarks
Model	7	2710.33	387.19	122.18	<0.0001	Highly significant
			646.87	204.12	<0.0001	Highly significant
A	1	24.51	24.51	7.73	0.012	Significant
B	1	2280.87	2280.87	719.72	<0.0001	Highly significant
C	1	159.43	159.43	50.31	<0.0001	Highly significant
D	1	122.69	122.69	38.71	<0.0001	Highly significant
A X A	1	34.59	56.29	17.76	<0.0001	Highly significant
B X B	1	75.71	75.71	23.89	<0.0001	Highly significant
Error	19	60.21	3.17			
Lack-of-Fit	17	60.21	3.54	6.24	0.547	Not Significant
Total	26	2770.54				

S	1.78020
R-sq	97.83%
R-sq(adj)	97.03%
R-sq(pred)	93.57%

269

270

271

272

273

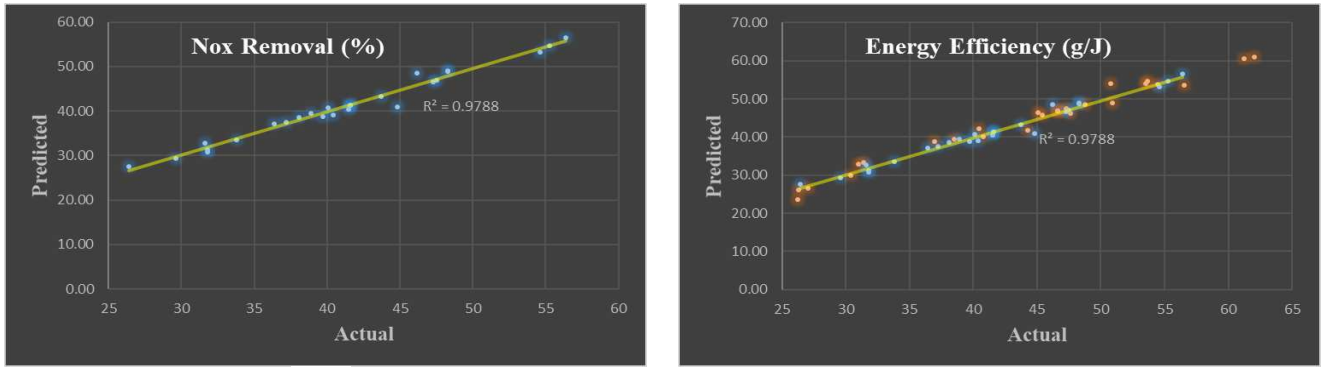

a b

Fig. 6 Actual vs Predicted plot a. NOx reduction and b. Energy Efficiency

Effect of independent variables on the responses

The two-dimensional contours shown in Fig. 7 and 8 examine the influence of the input factors in the DBD reactor, as seen in the BBD model, on NOx reductions and on the energy efficiency. Fig.s 7a, b and c examine the impact of two variables, with a different flow rate, voltage and electrode gap respectively, that the NOx concentration is set. The darker portion of Fig. 7a, b, and c show the greatest amount of nitrogen oxides removed, whilst the lightest part of Fig. 7b shows the lowest exclusion. In Fig. 7a, NOx concentration and gas flow rate are modified, while a central value of 25 kV and 4 mm respectively held the voltage and gap variable constant. These graphs demonstrate that rising NOx concentrations from 300 to 400 ppm and flow rates from 2 to 6 lpm results in a NOx reduction. With regard to Fig. 8a, however, increasing the NOx concentration and flow rate is more energy efficient. In equations (Eq 3-4), the flow improvement decreases energy density and, in essence, improves energy efficiency by enhancing gas flow (Shin et al. 2019). The greater the gas flow rate, the lower the gas holding duration in the reactor, leading to reductions in energy demand per unit mass and increased energy efficiency, leading to the decrease in NOx level. Similar findings are occurred in NOx deduction by plasma method as stated the researcher Shin et al. (2019).

The graphs 7b and 8b illustrate the effect of two variables, NOx concentration and voltage, on NOx reduction and energy efficiency. Because the voltage's value is so closely correlated with NOx concentration, it is apparent that this with respect to DBD revealed the DBD/NOx product voltage is the most dramatically influential. Additionally, the energy efficiency reduced as the voltage is increased in relation to the NOx concentration. Increased voltage greatly raises the energy density of micro discharge, which accelerates NOx reduction but reduces the DBD reactor's energy efficiency. The similar findings are stated several researchers (Aerts et al. 2015, Chen et al. 2017, Talebizadeh et al. 2014). It is also found that in the process of raising the voltage that the electron density in the gas triggered a further reaction (Eq 11-14), which took place in the plasma phase (Talebizadeh et al. 2014).

$$O_2 + e \rightarrow O + O + e \quad (11)$$

$$O_2 + O \rightarrow O_3 \quad (12)$$

$$NO + O \rightarrow NO_2 \quad (13)$$

$$NO + O_3 \rightarrow NO_2 + O_2 \quad (14)$$

After exciting phase, electrons are allowed to react with the mixture of oxygen, it is then split into two molecules and the component gases are then mixed, one of which is nitrous oxide and the other remained unreactive. This reinforced, unbroken, chain of environmental mechanisms has a much greater influence on NOx reduction capabilities. Specifically, O_3 has been shown to be an undesirable by product of many approaches to O_2 elimination. As an efficient generator, like O_3 causes the formation (such as NO_2) to occur, which affects the overall performance of the reaction phase (Wang et al. 2020). In addition to this, plasma enhanced NOx formation is another issue during the plasma aided NOx removal N_2O is regarded as the third most important greenhouse gas and the most significant stratospheric ozone diminishing substance (Tang et al. 2021).

The relationship among NOx concentration and electrode distance on NOx reduction and energy efficiency is depicted in Fig. 7c and 8c. Increases in the electrode gap as NOx concentration increased had a detrimental effect on NOx removal and energy production in the DBD reactor. It is discovered when a higher voltage applied to the outer electrode, as well as when a lower discharge gap is chosen, a lower voltage level is needed and thus better NOx removal could be accomplished with the same voltage (Vishal &Srihari 2020). Finally, reducing the electrode gap to 3 mm caused a significant increase in NOx removal reliability, because of the decrease in the discharge gap.

Fig. 7d shows the interrelationship of voltage to flow rate on NOx reduction with a given NOx concentration and distance of 350 ppm and 4 mm. Increasing the voltage as the flow rate increased had a beneficial effect on NOx reduction and energy consumption (Fig. 8d). Similarly, raising the flow rate with a distance has a negligible effect on energy efficiency (Fig. 8e), but the minimum flow rate with a small gap has the greatest effect on NOx reduction (Fig. 7e). Additionally, Fig. 7f illustrates the effect of increasing the voltage with an increase in the electrode gap on NOx reduction at a constant NOx concentration and flow rate, despite the fact that increasing the voltage with an increase in the electrode gap had a negative effect on NOx reduction. A similar finding is obtained for the DBD reactor's energy efficiency (Fig. 8f).

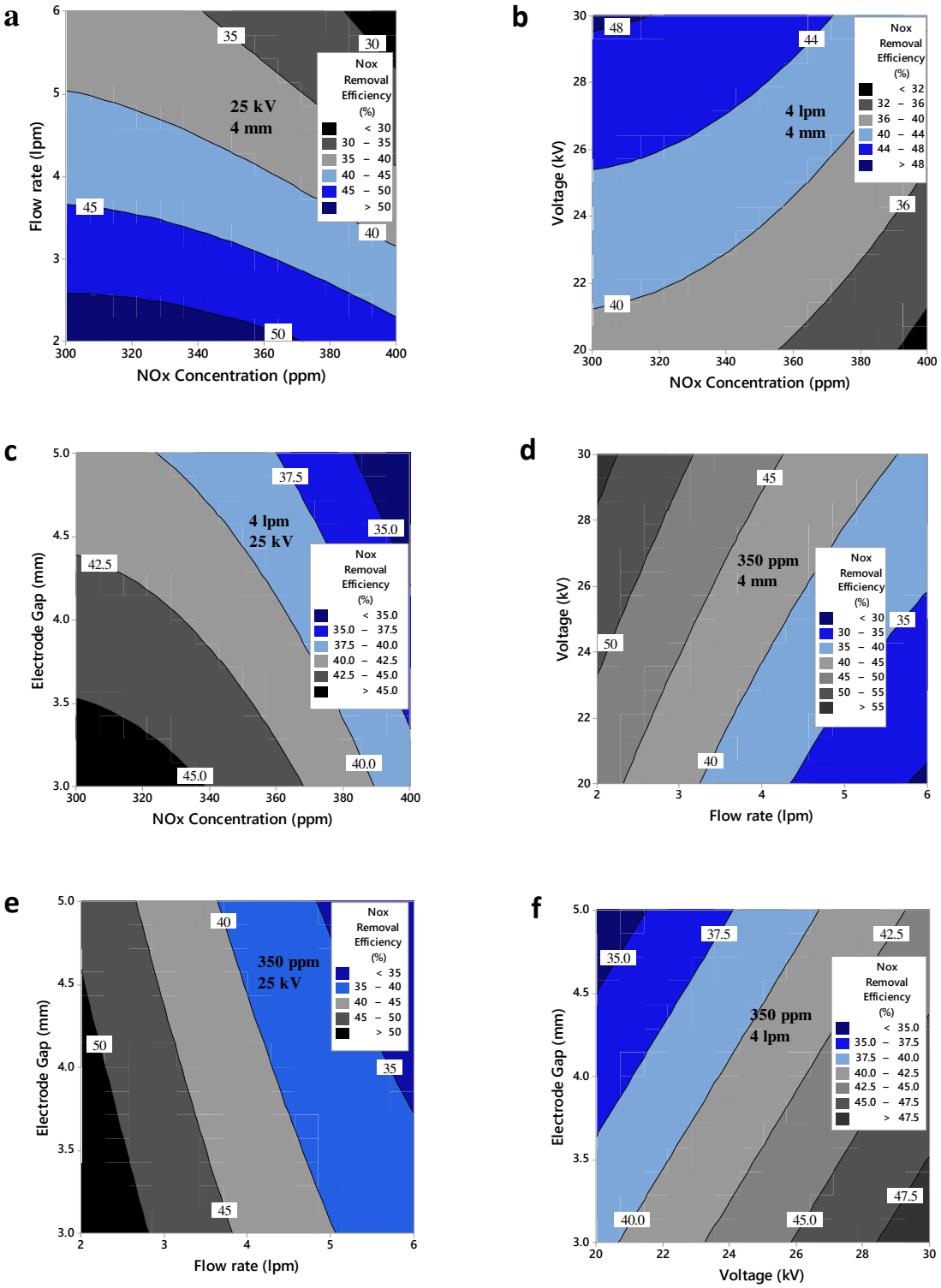

Fig. 7 Contour plot for NOx reduction a. flowrate vs NOx concentration, b. voltage vs NOx concentration, c. gap vs NOx concentration, d. voltage vs flowrate, e. gap vs flowrate and f. gap vs voltage

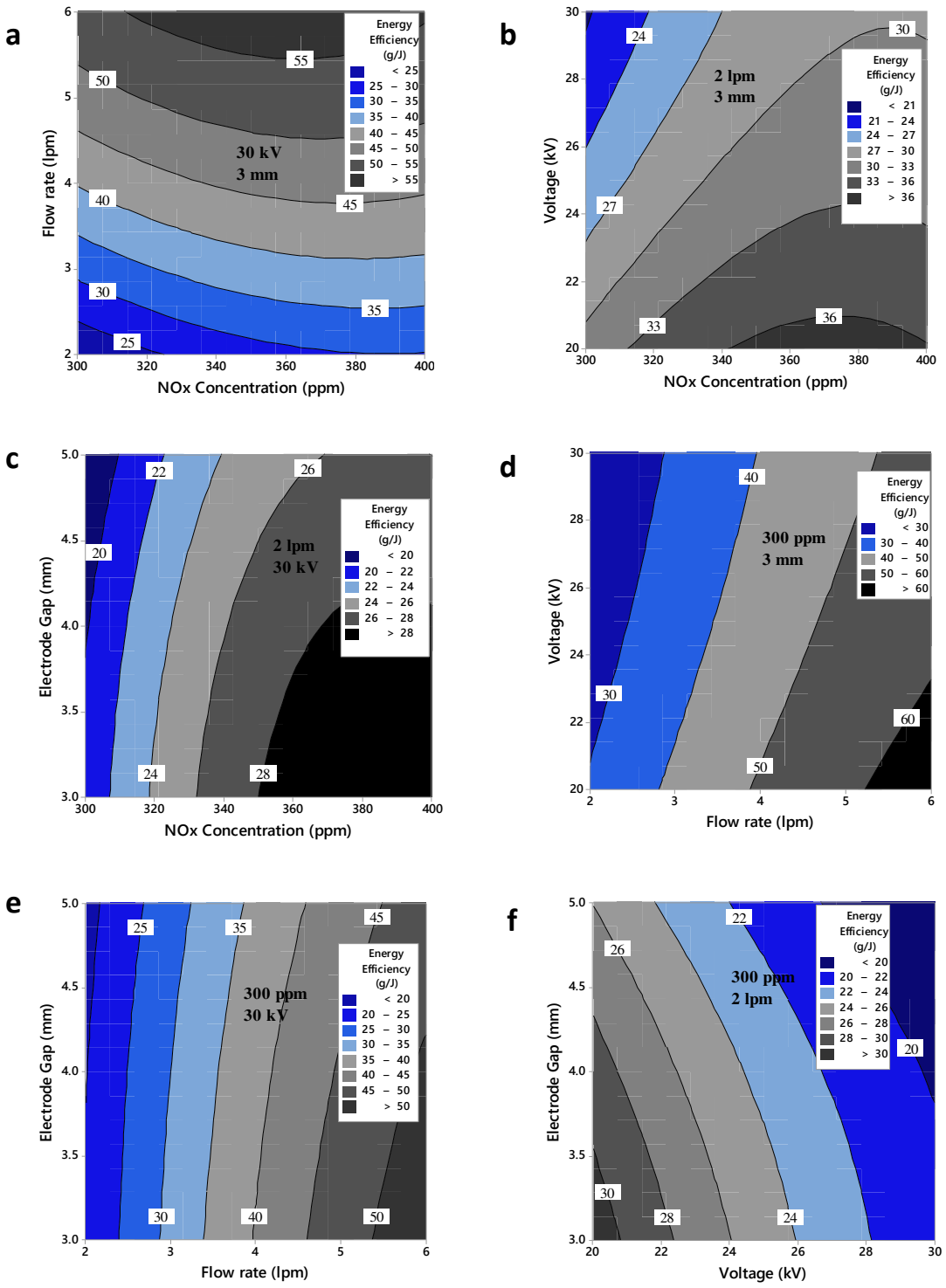

Fig. 8 Contour plot for energy efficiency a. flowrate vs NOx concentration, b. voltage vs NOx concentration, c. gap vs NOx concentration, d. voltage vs flowrate, e. gap vs flowrate and f. gap vs voltage

Optimum conditions

The maximum response is used as a benchmark for optimization concerning NOx reduction and energy efficiency, as well as other parameters including NOx concentration, flow rate, voltage, and electrode gap in the experimental study region. Using experimental trials, the optimal values obtained for NOx concentration, flow rate, voltage and voltage are presented in Table 6. As a result of this optimum condition, the overall NOx reduction is 60.5 % and the energy efficiency is 66.24 J/lit.

Table 4 Optimum conditions from BBD design

NOx Concentration (ppm)	Flow rate (lpm)	Voltage (kV)	Electrode gap (mm)	Result
NOx reduction				
300	2	30	3	60.5%
Energy Efficiency				
350	6	20	3	66.24 g/J

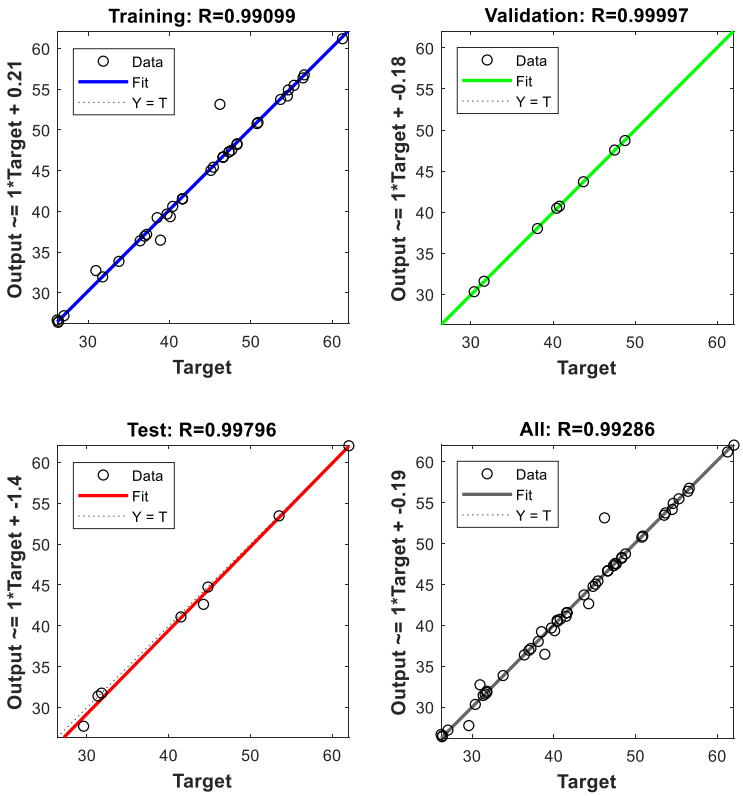

Fig. 9 ANN Regression plot

ANN modeling

ANN is used for the modelling and testing of the neuronal network model in NOx reduction experiments using the experimental results under the BBD operating conditions. To evaluate the optimal ANN model, a hidden layer of 1–14 neurons is used. Fig. 9 showed the preparation, evaluation, and test network performance curves along with their R-squared values for the R-terms (predictor-predicted), for comparison between all possible configurations of the network architectures. The accurate outcome presented here (network inputs equal output requirements) comes up with R=0.99. The findings show a strong association between the output values and goals during training (R=0.99099) and testing (R=0.9979). The results showed good correlations between output values and objectives. From Table 2 predicted findings are checked by the experimental data, confirming that the model had a good correlation with the actual result. Additional tests also demonstrate that the nonlinearity of the structure correctly as measured by the ANN model.

The "cause and effect" of the input variables is modelled by means of sensitivity analysis. Therefore, the system efficiency is determined to be improved by the results of the inputs of the predictor factors. In order to establish the value of the network variables for NOx reduction, the Garson equation and Connection weights algorithm have been employed. ANN given the coefficients, which stand for the interactions between inputs and outputs in an NTP reactor, each of which is calculated based on how much of the signal they received. The Garson equation and connection weights method are used to determine the relative influence of four input variables, as seen in Eq 15-16 (Goh 1995, Shin et al. 2019).

$$\mathrm{RI_G} = \frac{\sum_{n=1}^{k} |w_{mn} w_{nh}| / \sum_{t=1}^{v} |w_{tn}|}{\sum_{m=1}^{k} \sum_{n=1}^{k} (|w_{mn} w_{nh}| / \sum_{t=1}^{v} |w_{tn}|)} \quad (15)$$

$$\mathrm{RI_c} = \sum_{n=1}^{k} |w_{mn} w_{nh}| \quad (16)$$

Where, RI_G and RI_c denotes relative importance by garsons and connection weights algorithm, v and k denote number of hidden and input neurons, w_{mn} and w_{nh} denotes connection weight among input & hidden neuron and connection weight among hidden & output neuron.

In all cases, the findings show that all relation weights displayed positive or negative values, and in addition to being influenced. To prevent this, all relation weights have been determined in the adjusted Garson equation with their absolute value. Thus, the two approaches are compared on the end results, and tested based on the weights that are derived from preparation (Zhou et al. 2015). The changes in initial weights influenced the final weight. As seen in Table 5, the parameters are ranked according to their relative significance. This is based on the findings of the link weight process, which showed voltage is the most influential in the rate of reduction of NOx emission, followed by electrode distance and NOx concentration.

Table 5 Relative importance of input factors for NOx reduction

Input Variables	Connection Weight Method		Garson Method	
	Relative importance	Rank	Relative importance	Rank
NOx Concentration	16.98	4	2.33	3
Flow rate (lpm)	25.25	3	2.67	2
Voltage (kV)	32.28	1	2.68	1
Electrode Gap (mm)	28.42	2	2.32	4

In the data obtained by the Garson method (Table 11), it can be concluded that voltage and flow rate have the greatest effect on the removal rate, then NOx concentration and electrode gap, followed by NOx concentration. In terms of voltage and flow rate, this finding is not commensurate with the RSM result. The most important element (58,74% contribution) is that of voltage, according to the RSM model than flow rate (17.83 percent contribution). From this perspective, both flow rate and voltage have been the most critical variables, while electrode distance is the least critical. Garnson method is highly consistent with the BBD paradigm, according to this comparison of the relative value of ANN to BBD. Sensitivity analysis can quantify the proportion of effect, but the quadratic function describes the positive/negative correlation.

RSM and ANN model validation

Table 6 Comparision results for BBD and ANN

Response	Error	RSM	ANN
NOx Reduction	MSE	1.274	2.167
	RMSE	1.128	1.472
	MAPE	2.053	1.276
	R^2	0.98	0.99
Energy Efficiency	MSE	2.230	0.246
	RMSE	1.493	0.496
	MAPE	2.903	0.615
	R^2	0.97	0.99

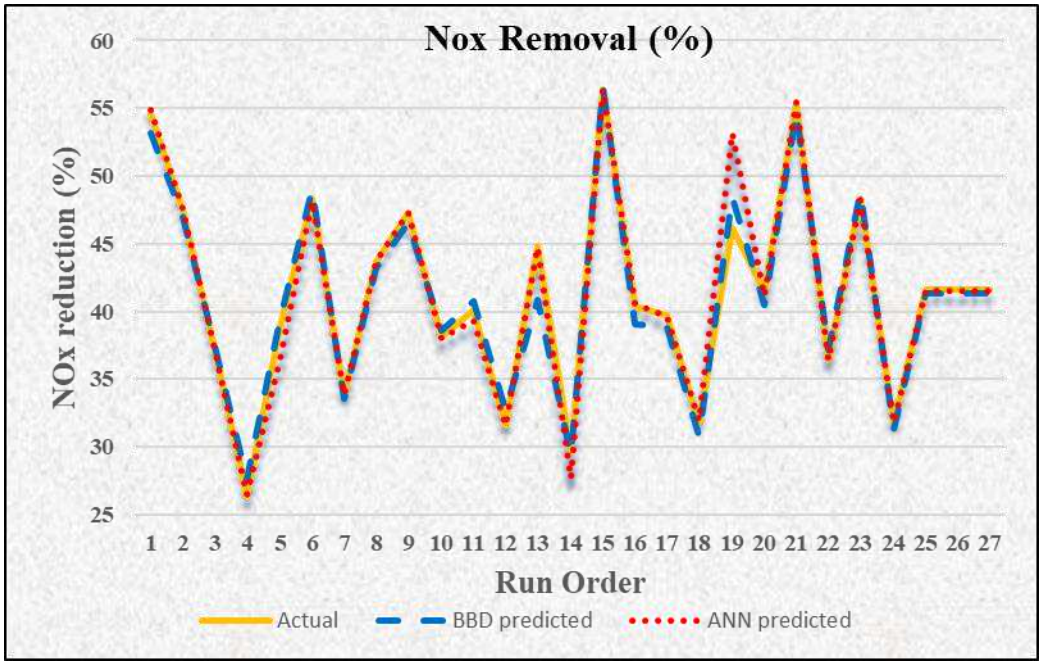

Fig. 10 Comparison plot for NOx reduction

The predictions, which are gathered from the experimentally observed responses, are compared to find out whether an ANN or an RSM approach is more efficient. The good use of R^2 values near 1.0, with the comparison of the statistic parameters acquired by ANN and RSM, are validated with the good usefulness of model's prediction. The findings of RSM and ANN experiments in NOx reduction and energy efficiency have been seen in Table 7, which compared their values to those of R^2, MSE, RMSE and MAPE. RSM Models NOx drop, R^2, MSE, RMSE and MAPE are respectively 0.98, 1.274, 1.128 and 2.053. In ANN, 0.99, 2.167.1.472 and 1.276 respectively for the R^2, MSE, RMSE and MAPE model. Similarly, the R^2, MSE, RMSE and MAPE values from the RSM models are respectively 0.97, 2.230, 1.493, and 2.903 for energy efficiency. A for ANN model, the R^2, MSE, RMSE and MAPE models included 0.99, 0.246, 0.46 and 0.615. It is found that the ANN models are more accurate than the RSM model at predicting the NOx removal/reduction and efficiency data. Fig. 10 depicts the distribution of experimental and predicted values of BBD and ANN model for NOx reduction of DBD system.

Conclusion

The experimentation was carried out in this study to limit NOx emissions from diesel engines using an NTP-based DBD reactor. The NOx elimination and energy efficiency of the DBD reactor have been modelled using Box Behnken Design (BBD) and Artificial Neural Network (ANN) techniques. Two approaches were used to optimise NOx concentration, gas flow rate, voltage and electrode gap parameters for reactor optimization of NOx reduction and energy efficiency. The current study's key conclusions can be outlined as follows:

- Contour plots have an effective means of analyzing factor relationships, as well as the final output model for the NTP process outlined 98.82% of variance in NOx reduction and 97.83% of the variation in energy efficiency. The plots show that the rise in the flow rate has been a strong factor in the reduction of NOx,

which has a direct effect on energy efficiency as the flow rate increases. Further, the voltage and electrode gap are positively correlated with NOx reduction but have a negative impact on energy efficiency.

- The optimum operating parameters of the NTP method was evaluated for NOx removal at NOx concentration of 300 ppm, voltage of 30 kV, electrode gap of 3 mm and flow rate of 2 lpm and for energy efficiency at NOx concentration of 350 ppm, voltage of 20 kV, electrode gap of 3 mm, and flow rate of 6 lpm. NOx removal was calculated to be 60.5% under these optimal conditions with an energy efficiency of 66.24 g/J.
- The validation experimental results showed that the ANN model (4-10-2) built from the minimal experimental data performed reasonably well. Furthermore, with a co-operative correlation coefficient of 0.99 for NOx reduction and energy efficiency, this model was capable of capturing the uncertainties of the experimental data stronger than the RSM model. As a result, the ANN model's accuracy in estimating the NOx removal process and in looking for the optimal condition was well than the RSM model. ANN explained it in terms of the relative importance of the various variables as listed higher to lower rank such as, voltage, flow rate, NOx concentration, and electrode gap on NOx reduction.
- These studies have led to potential outcomes in wide-ranging application of plasma technologies for the NOx removal.

Declarations

Ethics approval and consent to participate

Not applicable

Consent for publication

Not applicable

Availability of data and materials

Not applicable

Competing interests

We have no conflicts of interest to disclose.

Funding and Acknowledgements

We acknowledge that this project work was funded by UGC– Government of India under the scheme of Major research project (File No. 39-883/2010(SR)).

Authors' contributions

CM supervised and validated the whole project. ASR analyzed, interpreted and wrote the manuscript. RB helped in the ANN analyse. NS, RR and MV conducted the experiments.

References

Aerts R, Somers W, Bogaerts A (2015) Carbon dioxide splitting in a dielectric barrier discharge plasma: a combined experimental and computational study. ChemSusChem 8(4):702-16.

Agatonovic-Kustrin S, Beresford R (2000) Basic concepts of artificial neural network (ANN) modeling and its application in pharmaceutical research. Journal of pharmaceutical and biomedical analysis 22(5):717-727.

Amoatey P, Omidvarborna H, Baawain MS, Al-Mamun A (2019) Emissions and exposure assessments of SOX, NOX, PM10/2.5 and trace metals from oil industries:A review study (2000–2018). Process Safety and Environmental Protection 123:215-228.

Ansari M, Hossein Mahvi A, Hossein Salmani M, Sharifian M, Fallahzadeh H, Hassan Ehrampoush M (2020) Dielectric barrier discharge plasma combined with nano catalyst for aqueous amoxicillin removal:Performance modeling, kinetics and optimization study, energy yield, degradation pathway, and toxicity. Separation and Purification Technology 251:117270.

Armstrong RA, Eperjesi F, Gilmartin B (2002) The application of analysis of variance (ANOVA) to different experimental designs in optometry. Ophthalmic and Physiological Optics 22(3):248-256.

Arun kumar V, Krishnamurthy, K., Maheswari, C., Meenakshipriya, B., & Vinoth, R. (2019) Removal of NOX from diesel engine exhaust by using different chemical absorbent in a lab-scale packed column system. Journal of measurement and control 52(7):1095-1101.

Bhatti MS, Kapoor D, Kalia RK, Reddy AS, Thukral AK (2011) RSM and ANN modeling for electrocoagulation of copper from simulated wastewater:Multi objective optimization using genetic algorithm approach. Desalination 274(1):74-80.

Chen C-T, Tan W-L (2012) Mathematical modeling, optimal design and control of an SCR reactor for NOx removal. Journal of the Taiwan Institute of Chemical Engineers 43(3):409-419.

Chen JX, Pan KL, Yu SJ, Yen SY, Chang MB (2017) Combined fast selective reduction using Mn-based catalysts and nonthermal plasma for NOx removal. Environmental Science and Pollution Research 24(26):21496-21508.

Chen M, Liu Y (2010) NOx removal from vehicle emissions by functionality surface of asphalt road. Journal of Hazardous Materials 174(1):375-379.

Civelekoglu G, Yigit NO, Diamadopoulos E, Kitis M (2009) Modelling of COD removal in a biological wastewater treatment plant using adaptive neuro-fuzzy inference system and artificial neural network. Water Science and Technology 60(6):1475-1487.

Elmolla ES, Chaudhuri M, Eltoukhy MM (2010) The use of artificial neural network (ANN) for modeling of COD removal from antibiotic aqueous solution by the Fenton process. Journal of Hazardous Materials 179(1):127-134.

Goh AT (1995) Back-propagation neural networks for modeling complex systems. Artificial Intelligence in Engineering 9(3):143-151.

Kampa M, Castanas E (2008) Human health effects of air pollution. Environmental Pollution 151(2):362-367.

Keselman HJ, Huberty CJ, Lix LM, Olejnik S, Cribbie RA, Donahue B, Kowalchuk RK, Lowman LL, Petoskey MD, Keselman JC, Levin JR (1998) Statistical Practices of Educational Researchers:An Analysis of their ANOVA, MANOVA, and ANCOVA Analyses. Review of Educational Research 68(3):350-386.

Khan MSI, Kim Y-J (2020) Dielectric barrier discharge (DBD) plasma induced flavonoid degradation kinetics and mechanism in water. LWT 118:108777.

Kim Z, Shin Y, Yu J, Kim G, Hwang S (2019) Development of NOx removal process for LNG evaporation system:Comparative assessment between response surface methodology (RSM) and artificial neural network (ANN). Journal of Industrial and Engineering Chemistry 74:136-147.

Krosuri A, Wu S, Bashir MA, Walquist M (2021) Efficient degradation and mineralization of methylene blue via continuous-flow electrohydraulic plasma discharge. Journal of Water Process Engineering 40:101926.

Kuwahara T, Nakaguchi H, Kuroki T, Okubo M (2016) Continuous reduction of cyclic adsorbed and desorbed NOx in diesel emission using nonthermal plasma. Journal of Hazardous Materials 308:216-224.

Li Q, Yang H, Qiu F, Zhang X (2011) Promotional effects of carbon nanotubes on V2O5/TiO2 for NOX removal. Journal of Hazardous Materials 192(2):915-921.

Maheswari C, Priyanka E, Meenakshipriya B (2017) Fractional-order PIλDμ controller tuned by coefficient diagram method and particle swarm optimization algorithms for SO2 emission control process. Proceedings of the Institution of Mechanical Engineers, Part I:Journal of Systems and Control Engineering 231(8):587-599.

Maheswari C, Krishnamurthy, K & Parameshwaran, R (2014) Modelling and Experimental analysis of packed column for SO2 emission control process. Journal of Atmospheric pollution research 5(464- 470.

Maheswari C, Krishnamurthy, K & Parameshwaran, R (2013) Experimental Investigations on SO2 removal process using wet scrubber. Journal of Pollution research 32(3):655-662.
Mansouri F, Khavanin A, Jafari AJ, Asilian H, Ghomi HR, Mousavi SM (2020) Energy efficiency improvement in nitric oxide reduction by packed DBD plasma:optimization and modeling using response surface methodology(RSM). Environmental Science and Pollution Research 27(14):16100-16109.
McHugh ML (2011) Multiple comparison analysis testing in ANOVA. Biochemia medica 21(3):203-209.
Mizuno A (2007) Industrial applications of atmospheric non-thermal plasma in environmental remediation. Plasma Physics and Controlled Fusion 49(5A):A1-A15.
Mizuno A (2013) Generation of non-thermal plasma combined with catalysts and their application in environmental technology. Catalysis Today 211:2-8.
Picos-Benítez AR, López-Hincapié JD, Chávez-Ramírez AU, Rodríguez-García A (2017) Artificial intelligence based model for optimization of COD removal efficiency of an up-flow anaerobic sludge blanket reactor in the saline wastewater treatment. Water Science and Technology 75(6):1351-1361.
Sakiewicz P, Piotrowski K, Ober J, Karwot J (2020) Innovative artificial neural network approach for integrated biogas – wastewater treatment system modelling:Effect of plant operating parameters on process intensification. Renewable and Sustainable Energy Reviews 124:109784.
Shin Y, Kim Z, Yu J, Kim G, Hwang S (2019) Development of NOx reduction system utilizing artificial neural network (ANN) and genetic algorithm (GA). Journal of Cleaner Production 232:1418-1429.
Skalska K, Miller JS, Ledakowicz S (2010) Trends in NOx abatement:A review. Science of The Total Environment 408(19):3976-3989.
Sohn J, Hwang IS, Hwang J (2021) Improvement of ammonia mixing in an industrial scale selective catalytic reduction De-NOx system of a coal-fired power plant:A numerical analysis. Process Safety and Environmental Protection 147:334-345.
Soleimanzadeh H, Niaei A, Salari D, Tarjomannejad A, Penner S, Grünbacher M, Hosseini SA, Mousavi SM (2019) Modeling and optimization of V2O5/TiO2 nanocatalysts for NH3-Selective catalytic reduction (SCR) of NOx by RSM and ANN techniques. Journal of environmental management 238:360-367.
Srikanth H, Venkatesh J, Godiganur S (2021) Box-Behnken response surface methodology for optimization of process parameters for dairy washed milk scum biodiesel production. Biofuels 12(1):113-123.
Suresh R, Rajoo B, Chenniappan M, Palanichamy M (2021a):Treatment possibilities of electrical discharge non-thermal plasma for industrial wastewater treatment-review, IOP Conference Series:Materials Science and Engineering. IOP Publishing, pp. 012018
Suresh R, Rajoo B, Chenniappan M, Palanisamy M (2021b) Feasibility of applying nonthermal plasma for dairy effluent treatment and optimization of process parameters. Water and Environment Journal. 35:1038-50.
Takaki K, Shimizu M, Mukaigawa S, Fujiwara T (2004) Effect of electrode shape in dielectric barrier discharge plasma reactor for NOx removal. IEEE Transactions on Plasma Science 32(1):32-38.
Talebizadeh P, Babaie M, Brown R, Rahimzadeh H, Ristovski Z, Arai M (2014) The role of non-thermal plasma technique in NOx treatment:A review. Renewable and Sustainable Energy Reviews 40(886-901.
Tang X, Zhang R, Yi H, Gao F, Zhao S, Wang J, Yang K (2021) Byproducts Generation Characteristics of Non-thermal Plasma for NO Conversion:Effect of Reaction Conditions. Plasma Chemistry and Plasma Processing 41(1):369-387.
Vishal S, Srihari B (2020) Recent Advancements in Emission Reduction for Diesel Vehicles using Non Thermal Plasma Activation. International Journal of Innovative Science and Research Technology 5(5):1-7.
Wang B, Su H, Yao S (2020) Oxidation of NO with O3 under different conditions and the effects of SO2 and H2O vapor. Process Safety and Environmental Protection 133:216-223.
Zhao G, Li N, Li B, Li W, Liu Y, Chai T (2020) ANN model for predicting acrylonitrile wastewater degradation in supercritical water oxidation. Science of The Total Environment 704:135336.
Zhou B, Vogt RD, Lu X, Xu C, Zhu L, Shao X, Liu H, Xing M (2015) Relative importance analysis of a refined multi-parameter phosphorus index employed in a strongly agriculturally influenced watershed. Water, Air, & Soil Pollution 226(3):1-13.
Zhu T, Zhang X, Niu W, Liu Y, Yuan B, Li Z, Liu H (2020) Selective Catalytic Reduction of NO by NH3 Using a Combination of Non-Thermal Plasma and Mn-Cu/ZSM5 Catalyst. Catalysts 10(9):1044.
Zwanenburg G, Hoefsloot HCJ, Westerhuis JA, Jansen JJ, Smilde AK (2011) ANOVA–principal component analysis and ANOVA–simultaneous component analysis:a comparison. Journal of Chemometrics 25(10):561-567.